ARCHIVES OF MECHANICS
Arch. Mech. **72** (6), 525–553, 2020, DOI: 10.24423/aom.3598

Vertical heat transport at infinite Prandtl number for micropolar fluid

M. CAGGIO[1)], P. KALITA[2)], G. ŁUKASZEWICZ[3)], K. A. MIZERSKI[4)]

[1)] *Department of Information Engineering, Computer Science and Mathematics, University of L'Aquila, Via Vetoio, Coppito, 67100 L'Aquila, Italy, e-mails: matteo.caggio@univaq.it, matteocaggio@gmail.com*

[2)] *Faculty of Mathematics and Computer Science, Jagiellonian University, Łojasiewicza 6, 30-348 Kraków, Poland, e-mail: piotr.kalita@ii.uj.edu.pl*

[3)] *Institute of Applied Mathematics and Mechanics, University of Warsaw, Banacha 2, 02-097 Warsaw, Poland, e-mail: glukasz@mimuw.edu.pl*

[4)] *Department of Magnetism, Institute of Geophysics, Polish Academy of Sciences, Księcia Janusza 64, 01-452 Warsaw, Poland, e-mail: kamiz@igf.edu.pl*

We investigate the upper bound on the vertical heat transport in the fully 3D Rayleigh–Bénard convection problem at the infinite Prandtl number for a micropolar fluid. We obtain a bound, given by the cube root of the Rayleigh number, with a logarithmic correction. The derived bound is compared with the optimal known one for the Newtonian fluid. It follows that the (optimal) upper bound for the micropolar fluid is less than the corresponding bound for the Newtonian fluid at the same Rayleigh number. Moreover, strong microrotational diffusion effects can entirely suppress the heat transfer. In the Newtonian limit our purely analytical findings fully agree with estimates and scaling laws obtained from previous theories significantly relying on phenomenology.

Key words: micropolar fluid, Rayleigh–Benard convection, heat transport, Rayleigh number, Prandtl number, Nusselt number.

1. Introduction

The aim of this work is to investigate the vertical heat transport in the incompressible micropolar fluid. We consider the model of the Rayleigh-Bénard convection problem at the infinite Prandtl number. The micropolar model is both a simple and significant generalization of the Navier–Stokes model of classical hydrodynamics. It has much more applications than the classical model due to the fact that the latter cannot describe (by definition) fluids with microstructure. In general, individual particles of such complex fluids (e.g. polymeric suspensions, blood, liquid crystals) may be of different shape, may shrink

and expand or change their shape and moreover, they may rotate, independently of the rotation and movement of the fluid.

To describe accurately the behavior of such fluids one needs a theory that takes into account geometry, deformation, and intrinsic motion of individual material particles. In the framework of continuum mechanics several such theories have appeared, e.g., theories of simple microfluids, simple deformable directed fluids, micropolar fluids, dipolar fluids, to name some of them. To account for these local structural aspects, many classical concepts such as the symmetry of the stress tensor or absence of couple stresses have required a reexamination, and while many principles of classical continuum mechanics still remain valid for this new class of fluids, they had to be augmented with additional balance laws and constitutive relations. Some of these theories are very general, while others are concerned with special types of material structure and/or deformation; the potential applicability of the various theories is diverse. It is clear that each particular theory has its advantages as well as disadvantages when considered from a particular point of view. Some theories may seem more sound, logical, justifiable, and useful than others. None of them is universal.

One of the best-established theories of fluids with microstructure is the theory of micropolar fluids of [11] which has been mathematically studied by [17]. Physically, micropolar fluids may represent fluids consisting of rigid, randomly oriented (or spherical) particles suspended in a viscous medium, where the deformation of the particles is ignored. This constitutes a substantial generalization of the Navier–Stokes model and opens a new field of potential applications including a large number of complex fluids.

Let us point out some general features that make the model a useful tool in both theoretical studies and applications. The attractiveness and power of the model of micropolar fluids come from the fact that it is both a significant and a simple generalization of the classical Navier–Stokes model. Only one new vector field, the angular velocity field of rotation of particles, is introduced. Correspondingly, only one (vector) equation is added—it represents the conservation of the angular momentum. Although four new parameters, including three new viscosities and a micropolar moment of inertia are introduced, if one of them, namely the microrotation viscosity becomes zero, the conservation law of the linear momentum becomes independent of the presence of the microstructure. Thus, the size of the microrotation viscosity coefficient allows us to measure, in a certain sense, the deviation of flows of micropolar fluids from that of the Navier–Stokes model.

Owing to the simplicity of the model of micropolar fluids, in many classical applications (e.g. flows through the channel or between parallel plates) and under usual geometrical and dynamical assumptions made in such cases (e.g. symmetry, linearization of the equations), equations of micropolar fluids reduce to ones

that can be explicitly (i.e. analytically) solved. Thus the solutions obtained, depending on several parameters coming from the viscosity coefficients, can be easily compared with solutions of the corresponding problems for the Navier–Stokes equations. In addition, as several experiments show, the former solutions better represent behavior of numerous real fluids (e.g. blood) than corresponding solutions of the classical model, especially when the characteristic dimensions of the flow (e.g. the diameter of the channel) become small. It well agrees with our expectations that the influence of the internal structure of the fluid increases when the characteristic dimension of the flow is decreased.

The simplicity of the micropolar fluid model obviously does not mean mathematical triviality. The classical Navier–Stokes model itself, a special case of the micropolar fluid model, is far from being trivial. In this context simplicity means elegance and beauty of the mathematical theory.

The interest in the study of convection in micropolar fluids driven by a large vertical temperature jump across the fluid layer comes from the common applicability of the micropolar fluid model in lubrication theory and the industrial need for cooling abilities of lubricants, e.g. engine oils or refrigerant-oil mixtures in refrigeration compressors and vapor compression cooling systems [25, 16, 20]. Some non-Newtonian self-lubricating models of strongly viscous flows have also been used in geophysical modelling of natural convection in the Earth's mantle [3]. Other important applications of the considered model involve convective heat transfer in the flow of colloidal suspensions in chemical engineering and geophysics, e.g. hydrology and flow of river sediments, see [22, 5, 1] and references therein. Although there exists some numerical evidence that the vertical heat transfer measured by the Nusselt number, or at least its upper bound, decreases with increasing microrotational viscosity, see for instance [4, 6], the rigorous mathematical proof of this fact was incomplete: only the suboptimal bound for the finite Prandtl number which involves the square root of the Rayleigh number was obtained by [15]; moreover, [15] did not study the infinite Prandtl number limit and their findings concerned only the two-dimensional model of convection. The advantage of our analysis, is that it is fully three-dimensional and the estimate of the heat transfer at high Prandtl numbers is obtained in a fully mathematically rigorous manner. It is therefore a generalization of the Nusselt number bound obtained for Newtonian fluids by [10] to the case of micropolar fluids. Moreover, our estimate is in agreement with the effective theory of convection in Newtonian fluids developed in the seminal paper of [12] and later extended to high Prandtl number systems in [13]; the authors have systematized the knowledge and results from a vast number of previous experimental and numerical findings, to develop a consistent theory for scaling laws in turbulent convection. In this paper in Section 4 we suggest a way for generalization of the theory of [13] to non-Newtonian micropolar fluids, which is followed in Section 5

and appendicies by a rigorous derivation of an upper bound for the Nusselt number from first principles.

The plan of the paper is as follows. Section 2 is devoted to the formulation of the problem and statement of main result, Theorem 1. In Section 4 the theory of [12] is generalized to micropolar fluids and its prediction for a scaling law of the Nusselt number with the Rayleigh number is provided. The key idea of the proof of Theorem 1, namely the "background temperature profile method" is presented in Section 5. The method corresponds to the decomposition of the total temperature into an only vertically varying profile, which models the mean turbulent temperature profile, and a fluctuation. We end with some concluding remarks in Section 6. Majority of the technical details are presented in the appendices. In Appendix A we show, how the governing equations of micropolar fluid can be represented in Fourier modes. In Appendix B we prove an inequality, which directly corresponds to that of [10], cf. the inequality above (A.10) on p. 239 of that paper. The final Appendix C is devoted to the proof of the so-called spectral constraint, the key step in the proof of the Nusselt number upper bound.

We stress that the main points of the proof follow the method of [10], the key difference is that while in [10] there are obtained asymptotic estimates for the Rayleigh number Ra tending to infinity, we get the corresponding estimate for any finite Rayleigh number. Such a modification is needed as our aim is to demonstrate the diminishing effect of micropolar parameters on the Nusselt number upper bound at given fixed value of the Rayleigh number. In the proofs contained in appendices we stress only the differences between our argument and the one of [10]. These differences include the proof of inequality (B.1) presented in Appendix B, which in the Newtonian case is straightforward, and in micropolar one needs appropriate treatment of micropolar terms, and the proof of Corollary 5, where in Newtonian case the estimate of $|u_z''''|$ is obtained in just one step and in a micropolar case one needs auxiliary estimates of lower derivatives to get it.

2. Mathematical formulation and statement of the result

The governing (non-dimensional) system for the finite Prandtl number Pr is given by the following Boussinesq approximation for a micropolar fluid,

$$\frac{1}{\mathrm{Pr}}\left(\frac{\partial \mathbf{u}}{\partial t} + (\mathbf{u}\cdot\nabla)\mathbf{u}\right) + \nabla p = (1+K)\Delta\mathbf{u} + 2K\nabla\times\boldsymbol{\gamma} + \mathrm{Ra}\,\mathbf{k}T, \tag{2.1}$$

$$\nabla\cdot\mathbf{u} = 0, \tag{2.2}$$

$$\frac{M}{\mathrm{Pr}}\left(\frac{\partial \boldsymbol{\gamma}}{\partial t} + \mathbf{u}\cdot\nabla\boldsymbol{\gamma}\right) - L\Delta\boldsymbol{\gamma} - G\nabla(\nabla\cdot\boldsymbol{\gamma}) + 4K\boldsymbol{\gamma} = 2K\nabla\times\mathbf{u}, \tag{2.3}$$

$$\frac{\partial T}{\partial t} + \mathbf{u}\cdot\nabla T = \Delta T. \tag{2.4}$$

In the Boussinesq approximation the compressibility effects are neglected everywhere except for the buoyancy force and the thermal energy greatly exceeds the kinetic energy. In the above we have also neglected the effect of the adiabatic gradient, since in experimental situations the adiabatic gradient is typically a few orders of magnitude smaller than the temperature gradient which drives the flow (but we note, that in general convection is driven by the superadiabaticity, which plays an important role in large scale systems, such as e.g. the Earth's core, where most of the heat is conducted down the adiabat).

We assume that the space domain of the problem is the three-dimensional cuboid $\Omega = (0, l_1) \times (0, l_2) \times (0, 1)$ so that $|\Omega| = l_1 \cdot l_2$. The horizontal space variables are denoted by $x = (x_1, x_2)$, and the vertical one by z.

We set the standard periodic conditions at the lateral boundary, the following conditions at the top and bottom boundaries,

$$\mathbf{u}|_{z=0,1} = 0, \quad \boldsymbol{\gamma}|_{z=0,1} = 0, \tag{2.5}$$

$$T|_{z=0} = 1, \quad T|_{z=1} = 0, \tag{2.6}$$

and the initial conditions

$$T|_{t=0} = T_0, \quad \mathbf{u}|_{t=0} = \mathbf{u}_0, \quad \boldsymbol{\gamma}|_{t=0} = \boldsymbol{\gamma}_0. \tag{2.7}$$

Here, $\mathbf{u} = (u_{x_1}, u_{x_2}, u_z)$ and $\boldsymbol{\gamma} = (\boldsymbol{\gamma}_{x_1}, \boldsymbol{\gamma}_{x_2}, \boldsymbol{\gamma}_z)$ are the fluid velocity and the microrotation vector fields, p is the pressure, and T is the temperature. The vector $\mathbf{k}$ is the unit upward vector. Micropolar effects are described by the dimensionless parameters

$$K = \frac{\nu_r}{\nu}, \quad L = \frac{\alpha}{h^2\nu}, \quad G = \frac{\beta}{h^2\nu}, \quad M = \frac{j}{h^2}, \tag{2.8}$$

where ν_r and β are the first and second micropolar rotational viscosities, α is the couple stress parameter or micropolar damping, and j measures the micropolar moment of inertia. Values of these parameters for particular fluids have to be determined experimantally. For instance, for blood they depend on the hematocrit and this dependence has been presented in [2].

The system depends also on two dimensionless numbers: the Rayleigh number, Ra, which measures the relative strength of the buoyancy to damping effects, and the Prandtl number, Pr, that is the ratio of momentum diffusivity to thermal diffusivity, which are defined as follows

$$\mathrm{Ra} = \frac{g\tilde{\alpha}\Delta T h^3}{\chi\nu}, \quad \mathrm{Pr} = \frac{\nu}{\chi}. \tag{2.9}$$

In the above we have denoted the constant gravitational acceleration by g, the temperature jump across the layer by ΔT, and the thermal expansion coefficient of the fluid by $\tilde{\alpha}$.

To study flows at the large Prandtl number we may (formally) set the Prandtl number to be infinite. For the precise justification of such an operation for the Newtonian fluid see for example [24]. In our case we get the following (non-dimensional) system,

$$\nabla p = (1+K)\Delta \mathbf{u} + 2K\nabla \times \boldsymbol{\gamma} + \mathrm{Ra}\,\mathbf{k}T, \tag{2.10}$$

$$\nabla \cdot \mathbf{u} = 0, \tag{2.11}$$

$$-L\Delta\boldsymbol{\gamma} - G\nabla(\nabla\cdot\boldsymbol{\gamma}) + 4K\boldsymbol{\gamma} = 2K\nabla\times\mathbf{u}, \tag{2.12}$$

$$\frac{\partial T}{\partial t} + \mathbf{u}\cdot\nabla T = \Delta T \tag{2.13}$$

with boundary conditions (2.5), (2.6) and the initial condition (2.7) replaced by

$$T|_{t=0} = T_0. \tag{2.14}$$

However, we have to bear in mind, that the assumption $\mathrm{Pr}\to\infty$, which in real systems corresponds to $\mathrm{Pr}\gg 1$, has physical consequences. In general terms it means we assume that the viscous diffusion process is very fast compared to thermal diffusion, so that the time scale associated with viscous decay can be neglected. Consequently, it is important to realize, that when one assumes the other diffusion parameters K, L and G to be of order unity, this implies, that the times scales associated with micropolar diffusion processes h^2/ν_r, h^4/α and h^4/β are comparable with those for viscous diffusion, and hence are automatically removed from the dynamics. If necessary, these time scales could be retained by an additional assumption, that the three diffusion parameters K, L and G are much smaller than unity (of the order of Pr^{-1}). This would not alter Eq. (2.12), since all the terms in that equation would remain comparable but in the Navier–Stokes equation (2.10), K could then be neglected in comparison with unity next to the Laplacian. The term $2K\nabla\times\boldsymbol{\gamma}$ in (2.10), in general, needs to be retained in all cases, due to the possibility of formation of thin boundary layers i.e. regions of large velocity and $\boldsymbol{\gamma}$ gradients associated with the micropolar diffusion processes near the boundaries.

In the following analysis we make no assumptions regarding any of the four micropolar parameters in (2.8), so that in particular they may be considered to take values of the order unity.

Our aim is to estimate the Nusselt number Nu in terms of the Rayleigh number Ra and the micropolar parameters K and L, as well as to compare the estimate with that for the classical Boussinesq system for the corresponding Rayleigh–Bénard problem. Our result is the following

Theorem 1. *Assume that*

$$\widetilde{\mathrm{Ra}} = \mathrm{Ra}\left(\frac{4K+L}{4K+L+KL}\right) \geq 75.$$

Then there holds the bound

$$\mathrm{Nu} \le \frac{3}{\sqrt[3]{5}}\left[\mathrm{Ra}\left(\frac{4K+L}{4K+L+KL}\right)\right]^{1/3}\ln^{1/3}\left[\mathrm{Ra}\left(\frac{4K+L}{4K+L+KL}\right)\right].$$

Observe, that if K or L equals zero then the above estimate reduces, up to a prefactor, to one established for the Newtonian case [10] (if $K = L = 0$ the function multiplying Ra is undefined, if we set its value at $K = L = 0$ to 1, it stays continuous for $K \ge 0$ and $L \ge 0$). Our analysis remains valid for $K = 0$ so, for the Newtonian case it leads to the bound $\mathrm{Nu} \le 3/\sqrt[3]{5}\ \mathrm{Ra}^{1/3}\ln^{1/3}\mathrm{Ra}$ valid for $\mathrm{Ra} \ge 75$. We stress that the prefactor $3/\sqrt[3]{5}$ in Theorem 1 is valid for $\widetilde{\mathrm{Ra}} \ge 75$. The optimal prefactor $2/\sqrt[3]{30}$ is valid for $\widetilde{\mathrm{Ra}} \to \infty$, but as our aim is to demonstrate that increase of K and L decreases the Nusselt number upper bound, we choose to deal with the case of *finite* Rayleigh number, paying the price of the nonoptimal prefactor.

REMARK 1. Theorem 1 is valid, provided $\widetilde{\mathrm{Ra}} \ge 75$. If $\widetilde{\mathrm{Ra}} < 75$, taking $T(x,y,z,t) = \theta(x,y,z,t) + \tau(z)$ with the background $\tau(z) - 1 - z$ in (5.2) below, we obtain

$$\frac{1}{2}\frac{d}{dt}\|\theta(t)\|_{L^2}^2 + \|\nabla\theta\|_{L^2}^2 = (u_z,\theta) \le \|\mathbf{u}\|_{L^2}\|\theta\|_{L^2} \le \frac{1}{\pi^2}\|\nabla\mathbf{u}\|_{L^2}\|\nabla\theta\|_{L^2}, \tag{2.15}$$

where the Poincaré constant is given by $\frac{1}{\pi}$, cf. [15, Lemma 2.1]. Testing (2.10) by $\mathbf{u}$ and (2.13) by γ and adding the resulting equations we obtain

$$\|\nabla\mathbf{u}\|_{L^2}^2 + L\|\nabla\gamma\|_{L^2}^2 + K\|\nabla\mathbf{u} - 2\gamma\|_{L_2}^2 = \mathrm{Ra}(\theta, u_z).$$

Estimating, we obtain

$$\|\nabla\mathbf{u}\|_{L^2}^2 \le \mathrm{Ra}\,\frac{1}{\pi^2}\|\nabla\theta\|_{L^2}\|\nabla\mathbf{u}\|_{L^2},$$

whence

$$\|\nabla\mathbf{u}\|_{L^2} \le \mathrm{Ra}\,\frac{1}{\pi^2}\|\nabla\theta\|_{L^2}.$$

Using this bound in (2.15), we deduce

$$\frac{1}{2}\frac{d}{dt}\|\theta(t)\|_{L^2}^2 + \|\nabla\theta\|_{L^2}^2 = (u_z,\theta) \le \|\mathbf{u}\|_{L^2}\|\theta\|_{L^2} \le \mathrm{Ra}\,\frac{1}{\pi^4}\|\nabla\theta\|_{L^2}^2.$$

We see that if $\mathrm{Ra} < \pi^4$, then temperature converges to the purely condictive equilibrium and $\mathrm{Nu} = 1$. This includes the situation when $\widetilde{\mathrm{Ra}} < 75$.

3. Computation of Nu bound and boundary layer thickness

The proof of Theorem 1, contained in Appendix C, gives rise to an algorithm for the numerical computation of the optimal Nusselt number upper bound for a given value of $\widetilde{\mathrm{Ra}}$. While [10] derives only the asymptotic formulas valid for $\widetilde{\mathrm{Ra}} \to \infty$, we show how to calculate the Nusselt bound, which is optimal for the considered version of the background method and valid for particular $\widetilde{\mathrm{Ra}}$. The proof gives rise to the following optimization problem.

Find $\delta_0 \in A(\widetilde{\mathrm{Ra}})$ such that

$$\Phi(\delta_0) = \min_{\delta \in A(\widetilde{\mathrm{Ra}})} \Phi(\delta),$$

where

$$\Phi(\delta) = \frac{2}{\delta}\left(1 + \frac{\delta}{2\ln\frac{1-\delta}{\delta}} + \frac{1}{4\ln^2\frac{1-\delta}{\delta}}\left(1 - \frac{\delta}{1-\delta}\right)\right),$$

$$A(\widetilde{\mathrm{Ra}}) = \left\{\delta \in \left(0, \frac{1}{2}\right) : \int_0^\delta z^4\left(\frac{1}{\delta} + \frac{\lambda(\delta)}{z} + \frac{\lambda(\delta)}{1-z}\right)^2 dz \le \frac{4\lambda(\delta)}{\widetilde{\mathrm{Ra}}}\right\},$$

$$\lambda(\delta) = \frac{1}{2\ln((1-\delta)/\delta)}.$$

Once δ_0 is found, this number is the boundary later thickness, and $\Phi(\delta_0)$ is the optimal Nusselt number upper bound for $\widetilde{\mathrm{Ra}}$. After obtaining the analytic expression for the integral in the definition of $A(\widetilde{\mathrm{Ra}})$, the problem can be effectively approximated numerically. If we can verify that $\delta \in A(\widetilde{\mathrm{Ra}})$, then it is guaranteed that the Nusselt number is bounded from above by $\Phi(\delta)$. The implemented numerical solution realized in C++ with the use of CAPD interval arithmetic library ([14]) consists in searching the interval $(0, 1/2)$ for such $\delta \in A(\widetilde{\mathrm{Ra}})$ that $\Phi(\delta)$ is possibly lowest. After initial verification of all values of δ on an equidistant mesh of length 0.01, the candidate for solution is then refined using the bisection algorithm. Since the library CAPD works using the interval arithmetics which takes into account the rounding errors, the resultant Nu bound is guaranteed to be the upper bound of Nu for a given $\widetilde{\mathrm{Ra}}$. The results for several values of $\widetilde{\mathrm{Ra}}$ are presented in Table 1. The lowest bounds in the table come from [10], but the formulas there are asymptotic and valid only for $\widetilde{\mathrm{Ra}} \to \infty$, in the derivation of this bound all lower order terms are dropped. The remaining two bounds are valid for finite $\widetilde{\mathrm{Ra}}$. The optimal numerical bound is always smaller, in fact it is very close to the theoretical asymptotic bound but, to our knowledge, it cannot be expressed by a closed form formula. On the other hand, due to nonoptimal prefactor, the bound of Theorem 1 is always worst, it is about three times higher then the asymptotic bound. Still, it scales the same and has

the advantage of being given by the closed form formula. The relations between the bounds, the boundary layer thickness and $\widetilde{\mathrm{Ra}}$ in the range of $\widetilde{\mathrm{Ra}}$ 100–10000 are also depicted in Fig. 1. As expected, the asymptotic bound is always the lowest, the numerically calculated optimal bound for finite $\widetilde{\mathrm{Ra}}$ is a little bigger, and the bound obtained by the closed form formula for finite $\widetilde{\mathrm{Ra}}$ is the biggest.

Table 1. Bounds of Nu obtained from the optimization algorithm for various values of $\widetilde{\mathrm{Ra}}$. The results are compared with the bound of [10] and bound of Theorem 1. For the bound coming from the optimization algorithm, the associated value δ is the boundary layer thickness.

$\widetilde{\mathrm{Ra}}$	Nu bound from the optimization algorithm	δ	asymptotic Nu bound of [10]	Nu bound of Theorem 1
100	9.092	0.309674	4.971	13.55
1000	15.57	0.141878	12.26	33.42
10000	33.67	0.0619741	29.07	79.23
100000	75.25	0.0271865	67.47	183.9
1000000	168.9	0.0120132	154.5	421.0

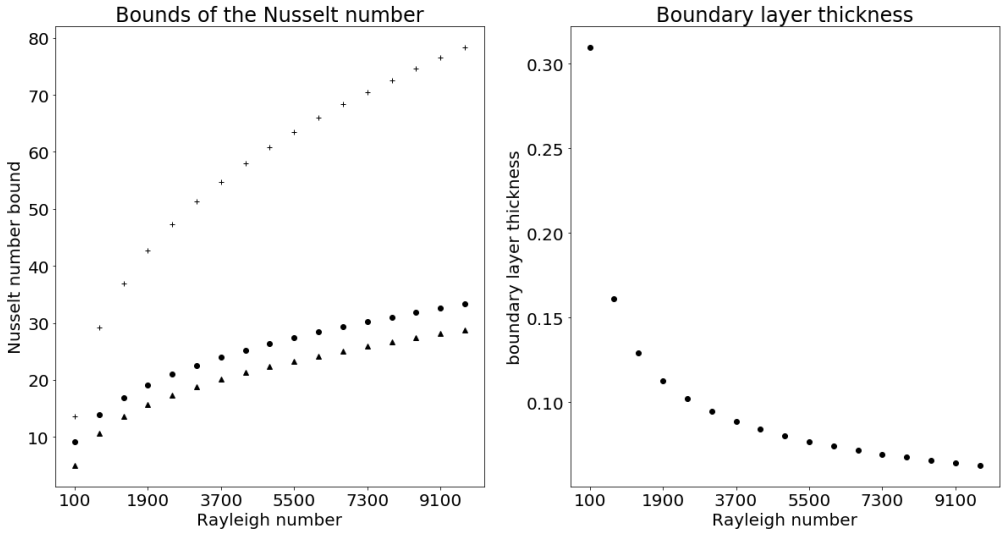

FIG. 1. Left plot presents three bounds of the Nusselt number as functions of the Rayleigh number $\widetilde{\mathrm{Ra}}$. Triangles depict the asymptotic bound of [10] which is the lowest, but it is valid only for $\widetilde{\mathrm{Ra}} \to \infty$. Circles represent the numerically calculated bound which is the best bound possible to obtain using this version of the background method. Finally, crosses present the bound obtained using Theorem 1. Although the bound found from the closed form formula of Theorem 1 is usually far from optimal, order of dependence on the Rayleigh number is the same as in the optimal bound. The right plot presents the boundary layer thickness δ as a function of $\widetilde{\mathrm{Ra}}$.

In the second numerical experiment we have calculated the optimal bound for a fixed finite Ra and various values of K and L. Results are presented in Table 2. In accordance with the expression on $\widetilde{\mathrm{Ra}}$ and the fact that optimal Nusselt bound is a monotone function of $\widetilde{\mathrm{Ra}}$ we observe the effect of decreasing the bound both with the increase of K as well as L.

Table 2. Bounds of Nu **obtained from the optimization algorithm for** $\mathrm{Ra} = 1000$ **and various values micropolar parameters** K **and** L**. Optimal value of** Nu **bound in the Newtonian case is equal to** 33.67**.**

	$L = 0.01$	$L = 0.1$	$L = 1$	$L = 10$	$L = 100$
$K = 0.01$	33.64	33.58	33.55	33.55	33.55
$K = 0.1$	33.64	33.44	32.87	32.61	32.58
$K = 1$	33.64	33.39	31.61	27.96	26.70
$K = 10$	33.64	33.38	31.22	23.11	16.61
$K = 100$	33.64	33.38	31.17	22.08	12.46

The plots of the dependence of the optimal Nusselt bound and boundary layer thickness for $\mathrm{Ra} = 1000$ on K and L are presented in Fig. 2. It is visible that increasing both L and K makes the Nusselt number bound smaller, and, as we expect from Theorem 1, the influence of L is stronger than that of K.

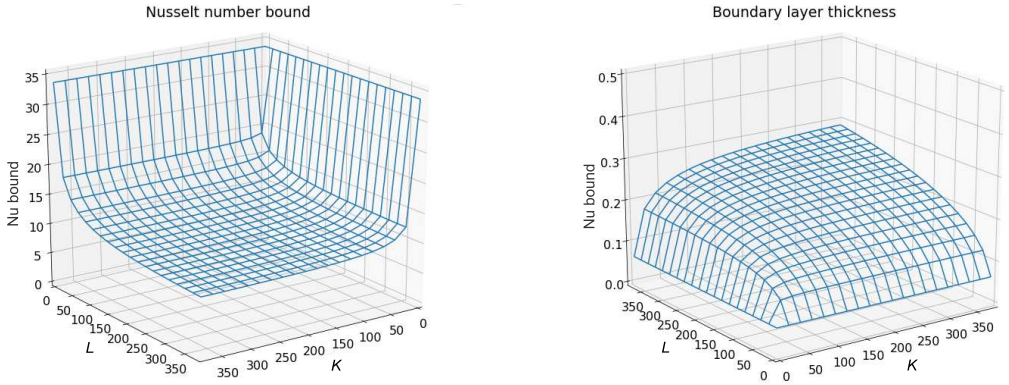

Fig. 2. Left plot presents the Nusselt number bound calculated by our algorithm as a function of micropolar parameters K and L for $\mathrm{Ra} = 1000$. Nu bound for the Newtonian case equals 33.67. Right plot depicts the corresponding boundary layer thickness. Different projections were used on both plots to make the surfaces more visible.

4. Relation to the theory of [12, 13] for developed, turbulent convection

We comment on the $\mathrm{Nu} \lesssim \mathrm{Ra}^{1/3}$ scaling law by the use of the theory of heat transport in developed turbulent, Boussinesq convection, originally developed

for Newtonian fluids in the comprehensive study of [12] (later updated in [23]), with the particular focus on the limit of infinite Prandtl number in [13][1]. To that end we introduce the Reynolds number

$$\mathrm{Re} = \frac{Uh}{\nu}, \tag{4.1}$$

where U, according to the central idea of the theory, is the magnitude of convective velocity in the coherent large scale convection roll, termed the "wind of turbulence". Such a large scale mean flow is an important characteristic of the turbulent Boussinesq convection, commonly observed in laboratory and numerical experiments, even at high Pr (although at large Pr the Reynolds number is small, the actual convective velocity, which is proportional to $\nu\,\mathrm{Pr}^{-1}\mathrm{Ra}^{2/3}$ is large, see discussion below (4.6)). We conjecture, that this feature persists in the case of convection, in micropolar fluids. Let us, for the time being, consider a statistically stationary state of a fully developed turbulence at the high Rayleigh number (we relax this assumption in the following sections). In order to obtain a clear correspondence with the approach of Grossmann and Lohse we also consider the dimensional form of the dynamical equations in this section

$$\nabla\frac{p}{\rho} = (\nu+\nu_r)\Delta\mathbf{u} + 2\nu_r\nabla\times\boldsymbol{\gamma} + g\tilde{\alpha}T\mathbf{k}, \tag{4.2a}$$

$$\nabla\cdot\mathbf{u} = 0, \tag{4.2b}$$

$$-\alpha\Delta\boldsymbol{\gamma} - \beta\nabla(\nabla\cdot\boldsymbol{\gamma}) + 4\nu_r\boldsymbol{\gamma} = 2\nu_r\nabla\times\mathbf{u}, \tag{4.2c}$$

$$\frac{\partial T}{\partial t} + \mathbf{u}\cdot\nabla T = \chi\Delta T. \tag{4.2d}$$

On multiplying Eq. (4.2a) by $\mathbf{u}$, Eq. (4.2c) by $\boldsymbol{\gamma}$ and Eq. (4.2d) by T and averaging over the entire periodic volume one obtains,

$$(\nu+\nu_r)\overline{\nabla\mathbf{u}:\nabla\mathbf{u}} - 2\nu_r\overline{\mathbf{u}\cdot\nabla\times\boldsymbol{\gamma}} = \frac{\nu^3}{h^4}\,\mathrm{Ra}(\mathrm{Nu}-1)\,\mathrm{Pr}^{-2}, \tag{4.3a}$$

$$\alpha\overline{\nabla\boldsymbol{\gamma}:\nabla\boldsymbol{\gamma}} + \beta\overline{(\nabla\cdot\boldsymbol{\gamma})^2} + 4\nu_r\overline{\boldsymbol{\gamma}^2} = 2\nu_r\overline{\boldsymbol{\gamma}\cdot\nabla\times\mathbf{u}}, \tag{4.3b}$$

$$\chi\overline{(\nabla T)^2} = \chi\frac{(\Delta T)^2}{h^2}\,\mathrm{Nu}, \tag{4.3c}$$

where the overbar denotes a volume average and the Nusselt number is defined in (5.3). Note, that in a stationary state the time average in the definition (5.3) is redundant. We introduce an additional assumption, that the magnitude of the

[1]Note, that the scaling law $\mathrm{Nu} \lesssim \mathrm{Ra}^{1/3}$ had been obtained much earlier, see e.g. [18, 19]. Later [13] have put it into the framework of their consistent theory of turbulent convection and explained the physical circumstances when this particular scaling law applies.

microrotation $\boldsymbol{\gamma}$ does not exceed the mean velocity gradient, i.e.

$$\|\boldsymbol{\gamma}\|_{L^2} \lesssim \frac{U}{h}. \tag{4.4}$$

Based on [12, 13] theory, in the limit of very large Prandtl number and large Rayleigh number so that convection is fully turbulent, the following estimates can be made

$$(\nu + \nu_r)\overline{\nabla \mathbf{u} : \nabla \mathbf{u}} \sim (\nu + \nu_r)\frac{U^2}{h^2} = \frac{\nu^3}{h^4}\,\mathrm{Re}^2(1+K), \tag{4.5a}$$

$$2\nu_r \overline{\boldsymbol{\gamma} \cdot \nabla \times \mathbf{u}} = 2\nu_r \overline{\mathbf{u} \cdot \nabla \times \boldsymbol{\gamma}} \lesssim 2\nu_r \frac{U^2}{h^2} = \frac{\nu^3}{h^4}\,\mathrm{Re}^2\,K, \tag{4.5b}$$

$$\chi\overline{(\nabla T)^2} \sim \frac{\delta}{h}\frac{U(\Delta T)^2}{h} \sim \chi\frac{(\Delta T)^2}{h^2}\,\mathrm{Re}\,\mathrm{Pr}\,\mathrm{Nu}^{-1}\,. \tag{4.5c}$$

Note, that Eq. (4.5b) simply provides a stationary balance between three different types of dissipative effects, that is the two micropolar rotational viscosities K and G and the micropolar damping L, but it does not affect the scaling exponent in the relation $\mathrm{Nu} \sim \mathrm{Ra}^n$. It is therefore expected that the final scaling law will match that of a Newtonian fluid. In Eq. (4.5c) we have used the standard estimate of the thickness of the thermal boundary layer $\delta \approx h/2\,\mathrm{Nu}$, valid for fully developed convection, which results from the symmetry of the Boussinesq system of equations with respect to the mid-plane and consequently the mean temperature profile in the form (5.1). The top and bottom boundary layers must, therefore, have the same thickness and the mean temperature in the bulk is uniform due to efficient convective mixing (cf. Fig. 3).

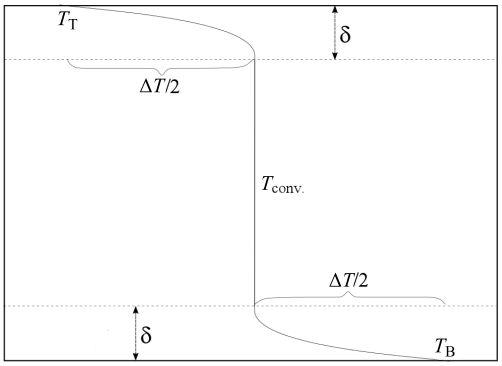

FIG. 3. Mean (horizontally averaged) temperature profile in developed Boussinesq convection. The efficient mixing in the bulk leads to a uniform mean temperature and formation of two boundary layers which adjust the bulk temperature to that of the boundaries. Due the the up-down symmetry of the Boussinesq system of equations the two boundary layers must have the same thickness. The mean heat flux can then be estimated as $\chi\rho c_p \Delta T/2\delta$, where ΔT is the temperature jump across the layer whereas ρ and c_p are the fluids density and specific heat at constant pressure respectively.

Equations (4.3a), (4.3c) and (4.5a-c) can be put together to yield

$$\mathrm{Re}^2\, f(K) \sim \mathrm{Ra}\,\mathrm{Nu}\,\mathrm{Pr}^{-2}, \qquad \mathrm{Nu}^4\,\mathrm{Pr}^{-2} \sim \mathrm{Re}^2, \tag{4.6}$$

where $f(K)$ is a function of the microrotation viscosity K and we have neglected unity with respect to the Nusselt number in (4.3a), since at large Rayleigh numbers the convection is turbulent and the convective heat flux greatly exceeds that of the hydrostatic solution. The two latter relations finally imply

$$\mathrm{Nu} \sim \mathrm{Ra}^{1/3}\, f(K)^{-1/3}. \tag{4.7}$$

This demonstrates the agreement between our estimate from the Theorem 1, which we rigorously prove in the following, and the theory of turbulent convection developed by [12, 13]. We note, however, that the relations (4.6) also yield $\mathrm{Re} \sim \mathrm{Ra}^{2/3}\,\mathrm{Pr}^{-1}\, f(K)^{-2/3}$, hence at very large Prandtl numbers the Reynolds number becomes small. Nevertheless, the mean convective velocity can be estimated as $U \sim \chi\,\mathrm{Ra}^{2/3}\, f(K)^{-2/3}/h$, thus implying vigorous convection. We also stress that choosing any inverse diffusive time scale, other than the eliminated viscous one, for the magnitude of the microrotation vector, such as e.g. χ/h^2, leads to $2\nu_r\overline{\boldsymbol{\gamma}\cdot\nabla\times\mathbf{u}} \sim (\nu^3/h^4)\,\mathrm{Re}\,K\chi/\nu$ and thus at large Pr this term becomes negligible in comparison with $(\nu+\nu_r)\overline{\nabla\mathbf{u}:\nabla\mathbf{u}}$ in (4.3a) leading to the same estimate for the Nusselt and Reynolds numbers. This demonstrates consistency with the assumption (4.4). Furthermore, it is of interest to note that at the smaller Rayleigh number the $\mathrm{Nu} \sim \mathrm{Ra}^{1/5}$ regime of [13] can also be obtained, which corresponds to the thermal dissipation taking place predominantly in the thermal boundary layers. Such a regime, of course, also satisfies the upper bound formulated in the Theorem 1. Finally, let us point out, that the dynamics would be significantly altered if the length scale associated with the microrotational moment of inertia were very small, i.e. $1/\sqrt{j} \ll h$, since this would also modify the possible dynamical time scales and of course reintroduce the inertial term in Eq. (2.3), thus invalidating the current theory. We therefore assume, that the length scale $1/\sqrt{j}$ is of comparable magnitude with the size of the fluid layer.

Note, that the precise form of the function $f(K)$ is unknown at this stage, however, in the following we demonstrate, that $f(K) \to \infty$ as both the micropolar rotational viscosity K and micropolar damping L increase to infinity (in the stationary state considered in this section K and L are related by (4.3b)). Consequently, the heat transfer in convection of a micropolar fluid can be almost entirely damped when the micropolar parameters are large.

5. The background temperature profile method

In this section we present the idea behind the background temperature profile method, associated with the homogenization of the boundary conditions for the

system of differential equations which allows to get rid of boundary integrals when dealing with energy methods.

In our case, to get the boundary conditions for the heat equation (2.13) homogeneous both on the bottom and top part of the boundary we introduce the so-called "background" temperature profile τ, which is a function $\tau : [0,1] \to \mathbb{R}$ of the variable z, such that $\tau(0) = 1$ and $\tau(1) = 0$, and we set

$$T(x,z,t) = \theta(x,z,t) + \tau(z). \tag{5.1}$$

Then, the "fluctuation" temperature θ satisfies homogeneous boundary conditions at $z = 0$ and $z = 1$, together with periodic boundary condition on the lateral boundaries.

With the above decomposition, Eq. (2.13) takes the form of a fluctuation evolution equation

$$\frac{\partial\theta}{\partial t} + \mathbf{u}\cdot\nabla\theta + u_z\tau'(z) = \Delta\theta + \tau''(z). \tag{5.2}$$

Now, the Nusselt number, the space-time averaged vertical heat flux, is given by

$$\mathrm{Nu} := 1 + \left\langle \int_\Omega u_z(x,z,t)T(x,z,t)\,dx\,dz \right\rangle \tag{5.3}$$

or, equivalently, see for example [8], by

$$\mathrm{Nu} := \left\langle \int_\Omega |\nabla T(x,z,t)|^2\,dx\,dz \right\rangle,$$

where $\langle\cdot\rangle$ denotes the time average defined by

$$\langle f\rangle = \limsup_{t\to\infty} \frac{1}{t}\int_0^t f(t')\,dt'.$$

The estimate of the Nusselt number is based on the analysis of Eq. (5.2). We observe that if the vertical component of the velocity field equals zero then $\mathrm{Nu} = 1$. This value of Nu corresponds in particular to the steady state solution of our problem $(\mathbf{u}, \boldsymbol{\gamma}, T) = (0, 0, 1 - z)$ and minimizes Nu over all solutions of the problem, see for example [8].

In order to establish an estimate of the Nusselt number, we test (5.2) by θ to get

$$\frac{1}{2}\frac{d}{dt}\|\theta(t)\|_{L^2}^2 + \|\nabla\theta\|_{L^2}^2 = (\tau'',\theta) - (u_z\tau',\theta), \tag{5.4}$$

and using the following relation between $\|\nabla\theta\|_{L^2}^2$ and $\|\nabla T\|_{L^2}^2$,

$$\|\nabla T\|_{L^2}^2 = \|\nabla\theta\|_{L^2}^2 - 2(\theta,\tau'') + \|\tau'\|_{L^2(0,1)}^2 \tag{5.5}$$

we obtain

$$\frac{1}{2}\frac{d}{dt}\|\theta(t)\|_{L^2}^2 + \frac{1}{2}Q(u_z(t),\theta(t),\tau) + \frac{1}{2}\|\nabla T(t)\|_{L^2}^2 = \frac{1}{2}\int_0^1 |\tau'(z)|^2\,dz, \tag{5.6}$$

where by $Q(u_z,\theta,\tau)$ we denoted the expression

$$Q(u_z,\theta,\tau) = \int_\Omega 2u_z(x,z)\tau'(z)\theta(x,z) + |\nabla\theta(x,z)|^2\,dx\,dz. \tag{5.7}$$

Now, if the "background" profile $\tau(z)$ is chosen such that

$$Q(u_z,\theta,\tau) \geq 0, \tag{5.8}$$

then, time averaging Eq. (5.6) and taking into account the boundedness of the L^2 norms of θ as a function of time which is a consequence of the maximum principle, we conclude that the Dirichlet integral of $\tau(z)$ is an upper bound for the Nusselt number, namely

$$\mathrm{Nu} \leq \int_0^1 |\tau'(z)|^2\,dz. \tag{5.9}$$

Thus, we reduced the upper estimate of the Nusselt number to the following variational problem: find

$$\inf_\tau\left\{\int_0^1 |\tau'(z)|^2\,dz : Q(u_z,\theta,\tau) \geq 0\right\}, \tag{5.10}$$

where the infimum is taken over all background profiles τ, and the constraint $Q(u_z,\theta,\tau) \geq 0$ is taken over a chosen functional space, say E, for $(\mathbf{u},\theta)$ such that E contains a solution of our problem.

This approach was used in [7] for the classical Boussinesq model, and by [15] for the micropolar fluids in the case of finite Prandtl numbers in the two-dimensional setting, giving an estimate of the form

$$\mathrm{Nu} \lesssim \mathrm{Ra}^{1/2}. \tag{5.11}$$

Since the infinite Prandtl models are simpler for mathematical investigation than

the finite ones, in this case it was possible to choose for E the set of solutions of the problem. Working with this minimal set in the context of finding the best background profile satisfying $Q(u_z, \theta, \tau) \geq 0$ led to a better estimate of Nu for this case, namely

$$\mathrm{Nu} \leq \mathrm{Ra}^{1/3} \times \text{logarithmic correction} \tag{5.12}$$

in the Newtonian case, see [10, 21]. The essence was to find possibly direct relations between u_z and θ as well as to use the physical knowledge of the temperature distribution in the Rayleigh–Bénard convection problem when choosing the temperature profile τ. Application of Fourier analysis allowed to eliminate the integral in the horizontal variables from the expression for Q and to obtain a relation between Fourier modes in the vertical variable of $\mathbf{u}$ and θ in the form of a a system of ordinary differential equations.

Writing the constraint (5.8) in terms of Fourier modes, and omiting the time parameter t, it suffices to prove that

$$\int_0^1 \left\{ \tau'(z)(\widehat{u}_k(z)\overline{\widehat{\theta}_k(z)} + \overline{\widehat{u}_k(z)}\widehat{\theta}_k(z)) + |k|^2|\widehat{\theta}_k(z)|^2 + |\widehat{\theta}_k'(z)|^2 \right\} dz \geq 0 \tag{5.13}$$

holds for every $k \in \mathbb{Z}$.

It is possible to show (see Appendix A) that the Fourier modes $\widehat{u}_k$ and $\widehat{\theta}_k$ satisfy the following relations,

$$(1+K)(k^4\widehat{u}_k - 2k^2\widehat{u}_k'' + \widehat{u}_k'''') + 2K(k^2\widehat{\zeta}_k - \widehat{\zeta}_k'') = \mathrm{Ra}\, k^2\widehat{\theta}_k, \tag{5.14}$$

$$L(k^2\widehat{\zeta}_k - \widehat{\zeta}_k'') + 4K\widehat{\zeta}_k + 2K(k^2\widehat{u}_k - \widehat{u}_k'') = 0, \tag{5.15}$$

equipped with the boundary conditions

$$\widehat{u}_k(0) = \widehat{u}_k(1) = \widehat{u}_k'(0) = \widehat{u}_k'(1) = \widehat{\zeta}_k(0) = \widehat{\zeta}_k(1) = 0, \tag{5.16}$$

where $\widehat{\zeta}_k$ is the k-th Fourier mode of the third component of rotation of the microrotation vector field, namely,

$$\zeta = \frac{\partial \boldsymbol{\gamma}_{x_2}}{\partial x_1} - \frac{\partial \boldsymbol{\gamma}_{x_1}}{\partial x_2}.$$

Comparing (5.7) and (5.13) we can see that (5.9) is satisfied if only

$$\int_0^1 \left\{ 2\tau'(z)\,\mathrm{Re}[\overline{\widehat{u}_k(z)}\widehat{\theta}_k(z)] + |\widehat{\theta}_k'(z)|^2 \right\} dz \geq 0 \tag{5.17}$$

holds for every $k \in \mathbb{Z}$ (note that here and hereafter Re denotes the real part of the complex number). In fact, it is sufficient to prove this bound for every $k \in \mathbb{Z} \setminus \{0\}$ as for $k = 0$ the unique solution of (5.14)–(5.15) with boundary conditions (5.16) is $\widehat{u}_0(z) = 0$ and $\widehat{\zeta}_0(z) = 0$, and the bound follows trivially.

Our aim is to obtain an upper bound of the Nusselt number for the micropolar case of the form (5.12), thus the same form as for the Newtonian model, but with a modified Rayleigh number which takes into account the micropolar model parameters, cf. Theorem 1. We shall prove that in the final analysis we can proceed exactly in the same framework as [10] using the so-called logarithmic background profile. As it is shown, the main idea for the application of the background profile is to choose $\tau(z)$ such that $\tau' \simeq 0$ in the bulk of the fluid, plus the introduction of "thin" boundary layers. With this choice, $Q(u_z, \theta, \tau)$ is increasingly positive as the width of the boundary layers decreases, but the Dirichlet integral of $\tau(z)$ is also increasing. The problem is to minimize the Dirichlet integral of $\tau(z)$ under the constraint that $Q(u_z, \theta, \tau)$ is a non-negative quadratic form. In the framework of [10] we introduce a class of logarithmic background profiles where $\tau(z) \simeq \ln z$ in the bulk so that $\tau'(z) \simeq z^{-1}$. Consequently, the "stable" stratification in the bulk that increases the Dirichlet integral of $\tau(z)$ will be compensated by the contribution from $z^{-1}\mathrm{Re}\,[\theta\overline{u_z}]$ in the bulk to the positivity of $Q(u_z, \theta, \tau)$. The details of the proof of Theorem 1 are moved to Appendices B and C. Namely, the proof of an auxiliary inequality (B.1), crucial for the proof, which corresponds to the inequality (A.10) of [10] is presented in Appendix B, while the proof of the spectral constraint (5.17) and the calculation of the Nusselt number bound are resented in Appendix C. For brevity, only those parts of the proof which differ from that of [10] are described in detail.

6. Conclusions

We have derived an estimate of the Nusselt number for convectively driven flows of non-Newtonian, micropolar fluids at a high Prandtl number. The advantage of the presented approach is that our fully rigorous derivations are conducted in three dimensions, as opposed to our previous findings, [15], which considered only two-dimensional convection. This is of significance, since rigorous derivations in three-dimensions are rather rare due to its high complexity and it is known that the properties of fully three-dimesional turbulence are often fundamentally different from those of the 2D case. Our theory is applied to an important generalization of fluid models, that is the micropolar fluids, which include microstructural effects. The limit of Newtonian fluids is easily obtained by setting just one parameter to zero, i.e. the first micropolar rotational viscosity, $\nu_r = 0$. Furthermore, we have also proposed a way to generalize the theory of turbulent convection of Grossman and Lohse (2000, 2001), which was based on

a mixed analytical-phenomenological approach, to the case of micropolar fluids. Indeed, our rigorous estimate provided in the Theorem 1 agrees with the scaling law $\mathrm{Nu} \sim \mathrm{Ra}^{1/3}$ predicted by the theory likewise the laboratory and numerical experiments in the Newtonian fluid limit. An important conclusion that can be drawn from the obtained estimate is that the heat transfer in three-dimensional convection of a micropolar fluid can be almost entirely suppressed when the micropolar rotational viscosity K and the micropolar damping L are large (cf. the estimate in Theorem 1). The obtained result is significant from the point of view of the lubrication theory, where micropolar fluids are often used to model lubricants. The common and important industrial applications of the lubrication theory involve the problem of cooling of engines or heat transfer in refrigeration compressors.

We can see from the above argument that the method of background profile is rather crude. In this method the spectral constrain is supposed to be satisfied by all functions which can be admissible as the problem solutions. We know, thanks to the dissipativity of the system, properties of the flow improve with time and that thanks to the boundedness in time of the integrand in the definition of the Nusselt number the latter does not depend on any finite time interval $[0, a]$. It is thus strange that we obtain expected results (for the Newtonian case they are confirmed by experiments). Working with solutions as the set E improves the estimates, however, in the Fourier analysis we simplify in several places, for example, in the spectral constraint we demand every mode to be nonnegative, and not their sum. It would be something really original to verify if the time asymptotics of solutions could lead to better estimates of Nu. We have studied the dependence of the Nusselt number bound on micropolar parameters for micropolar fluids. We leave as an interesting open question the issue if effects of microstructure decrease the Nusselt number bound for other classes of fluids. In particular it would be interesting to investigate heat transfer in fluids where the particles could deform.

Acknowledgements

Work of P.K. and G.Ł. was supported by National Science Center (NCN) of Poland under the project No. DEC-2017/25/B/ST1/00302, work of P.K. was also partially supported by NCN of Poland under the project No. UMO-2016/22/A/ST1/00077. The first version of the paper was done during the stay of M.C. at the Institute of Mathematics, Academy of Sciences of the Czech Republic and was supported by the project GA16-03230S. Partial support of the Ministry of Science and Higher Education of Poland within statutory activities No 3841/E-41/S/2018 and of the Polish National Science Centre (Grant No 2017/26/E/ST3/00554) is gratefully acknowledged.

Appendix A. Relations between Fourier modes

The aim of this section is to prove relations (5.14)–(5.15) between Fourier modes $\widehat{u}_k, \widehat{\theta}_k$ appearing in the spectral constraint (5.17), and the modes $\widehat{\zeta}_k$. This involves some operations on the original system of equations (2.10)–(2.12).

First, we eliminate the pressure and the horizontal component of the velocity vector field from the system. We differentiate the first equation in (2.10) with respect to x_1 and z, the second equation with respect to x_2 and z, add thus obtained equations to each other and then subtract the third equation in (2.10) after applying to it the horizontal Laplacian

$$\Delta_H = \frac{\partial^2}{\partial x_1^2} + \frac{\partial^2}{\partial x_2^2}.$$

Making use of the incompressibility condition in the end we obtain

$$(1+K)\Delta^2 u_z + 2K\Delta\zeta = -\operatorname{Ra}\Delta_H T = -\operatorname{Ra}\Delta_H\theta.$$

Next, we differentiate the second equation in (2.12) with respect to x_1 and subtract from thus obtained equation the first equation in (2.12) differentiated with respect to x_2. Using the incompressibility condition, we obtain

$$-L\Delta\zeta + 4K\zeta + 2K\Delta u_z = 0.$$

In this way we obtained the following system of equations

$$(1+K)\Delta^2 u_z + 2K\Delta\zeta = -\operatorname{Ra}\Delta_H\theta, \tag{A.1}$$

$$-L\Delta\zeta + 4K\zeta + 2K\Delta u_z = 0, \tag{A.2}$$

where u_z and ζ are $[l_1, l_2]$-periodic at the lateral boundaries. From the incompressibility condition we have $\zeta = u_z = \nabla u_z = 0$ at the top and bottom boundaries. As the conditions on the lateral boundaries are periodic, we can express u_z, θ, and ζ as the sum of the Fourier series in the horizontal direction, namely

$$u_z = \sum_k e^{ik\cdot x}\widehat{u}_k(z), \quad \zeta = \sum_k e^{ik\cdot x}\widehat{\zeta}_k(z), \quad \theta = \sum_k e^{ik\cdot x}\widehat{\theta}_k(z). \tag{A.3}$$

The summation is over all wavenumbers $k = 2\pi n_1/l_1$, $k = 2\pi n_2/l_2$ where $n = (n_1, n_2) \in \mathbb{Z}^2$. Moreover, we have the conditions $\widehat{u}_k = \overline{\widehat{u}_{-k}}$, $\widehat{\zeta}_k = \overline{\widehat{\zeta}_{-k}}$ and $\widehat{\theta}_k = \overline{\widehat{\theta}_{-k}}$, which guarantee that the result of the summation is real.

Rewriting (A.1)–(A.2) in terms of horizontally Fourier transformed variables, we obtain the following infinite system of independent ODEs

$$(1+K)\left(|k|^2 - \frac{d^2}{dz^2}\right)^2\widehat{u}_k + 2K\left(|k|^2 - \frac{d^2}{dz^2}\right)\widehat{\zeta}_k = \operatorname{Ra}|k|^2\widehat{\theta}_k,$$

$$L\left(|k|^2 - \frac{d^2}{dz^2}\right)\widehat{\zeta}_k + 4K\widehat{\zeta}_k + 2K\left(|k|^2 - \frac{d^2}{dz^2}\right)\widehat{u}_k = 0,$$

which is thus another form of (5.14)–(5.15).

The constraint (5.8) written in terms of the Fourier representation (A.3) reads

$$\sum_k \int_0^1 2\tau'(z)(\widehat{u}_k(z)\overline{\widehat{\theta}_k(z)} + \overline{\widehat{u}_k(z)}\widehat{\theta}_k(z)) + |k|^2|\widehat{\theta}_k(z)|^2 + |\widehat{\theta}_k'(z)|^2\,dz \geq 0. \tag{A.4}$$

Appendix B. An auxiliary inequality

In this section we shall prove the following inequality

$$\frac{2}{\widetilde{\mathrm{Ra}}}\Big(|\sqrt{z}\varphi|\,|\sqrt{z}\varphi''| + |\sqrt{z}\varphi'|^2\Big) \leq \mathrm{Re}(\theta, \overline{\varphi}), \tag{B.1}$$

where

$$\widetilde{\mathrm{Ra}} = \mathrm{Ra}\,\frac{4K+L}{4K+L+KL} \tag{B.2}$$

and

$$\varphi := \frac{u_z}{z}, \quad \psi := \frac{\zeta}{z}.$$

Having this inequality the problem of proving the upper bound of the Nusselt number for the micropolar Boussinesq model of the form (5.12) is then reduced to the analysis performed in [10] with Ra replaced with $\widetilde{\mathrm{Ra}}$, where $\widetilde{\mathrm{Ra}}$ plays the same role as Ra in further computations. Note that

$$\widetilde{\mathrm{Ra}} = \mathrm{Ra}\,\frac{4K+L}{4K+L+KL} \leq \mathrm{Ra} \tag{B.3}$$

and that $\widetilde{\mathrm{Ra}}$ is always smaller than Ra if K, L are positive, equal to Ra if $K = 0$ or $L = 0$, and it can be made arbitrarily small by taking large L and K.

To obtain (B.1) we rewrite Eqs. (5.14)–(5.15) in a simpler notation as

$$(1+K)(k^4 u_z - 2k^2 u_z'' + u_z'''') + 2K(k^2\zeta - \zeta'') = \mathrm{Ra}\,k^2\theta, \tag{B.4}$$

$$L(k^2\zeta - \zeta'') + 4K\zeta + 2K(k^2 u_z - u_z'') = 0, \tag{B.5}$$

$$u_z(0) = u_z(1) = u_z'(0) = u_z'(1) = \zeta(0) = \zeta(1) = 0. \tag{B.6}$$

Moreover, from now on, to make the computations more brief we denote by $|\cdot|$ the L^2 norm, namely

$$|f| = \sqrt{\int_0^1 |f(z)|^2\,dz}$$

and write k^2 instead $|k|^2$.

Now, we multiply (B.4) by $\overline{\varphi} = \overline{u_z}/z$. After integration over the interval $(0,1)$, we obtain

$$(1+K)(k^4|\sqrt{z}\varphi|^2 + 2k^2|\sqrt{z}\varphi'|^2 + |\sqrt{z}\varphi''|^2) + 2K\,\mathrm{Re}(k^2(\zeta,\overline{\varphi}) - (\zeta'',\overline{\varphi})) = \mathrm{Ra}\,k^2\,\mathrm{Re}(\theta,\overline{\varphi}). \tag{B.7}$$

We multiply (B.5) by $\overline{\psi} = \overline{\zeta}/z$. After integration over the interval $(0,1)$, we obtain

$$L|\sqrt{z}\psi'|^2+(Lk^2+4K)|\sqrt{z}\psi|^2+2K\,\mathrm{Re}(k^2(z\varphi,\overline{\psi})+(z\varphi',\overline{\psi}')+(\varphi',\overline{\psi})) = 0, \tag{B.8}$$

where we observed

$$-\left(u'', \frac{\overline{\zeta}}{z}\right) = (z\varphi', \overline{\psi}') + (\varphi', \overline{\psi}).$$

From (B.7) it follows that

$$(1+K)(k^4|\sqrt{z}\varphi|^2 + 2k^2|\sqrt{z}\varphi'|^2 + |\sqrt{z}\varphi''|^2) + 2K\,\mathrm{Re}(k^2(z\psi,\overline{\varphi}) - ((z\psi)'',\overline{\varphi})) = \mathrm{Ra}\,k^2\,\mathrm{Re}(\theta,\overline{\varphi}). \tag{B.9}$$

Observing that

$$-((z\psi)'',\overline{\varphi}) = (z\psi',\overline{\varphi}') + (\psi,\overline{\varphi}'),$$

implies the equation

$$(1+K)(k^4|\sqrt{z}\varphi|^2 + 2k^2|\sqrt{z}\varphi'|^2 + |\sqrt{z}\varphi''|^2) + 2K\,\mathrm{Re}(k^2(z\psi,\overline{\varphi}) + (z\psi',\overline{\varphi}') + (\psi,\overline{\varphi}')) = \mathrm{Ra}\,k^2\,\mathrm{Re}(\theta,\overline{\varphi}). \tag{B.10}$$

Now, adding (B.8) to (B.10), we obtain

$$\begin{aligned}(1+K)(k^4|\sqrt{z}\varphi|^2 + 2k^2|\sqrt{z}\varphi'|^2 + |\sqrt{z}\varphi''|^2) + L|\sqrt{z}\psi'|^2 \\ + (Lk^2+4K)|\sqrt{z}\psi|^2 + 2K(k^2(z\psi,\overline{\varphi}) + (z\psi',\overline{\varphi}') \\ + (\psi,\overline{\varphi}') + k^2(z\varphi,\overline{\psi}) + (z\varphi',\overline{\psi}') + (\varphi',\overline{\psi})) = \mathrm{Ra}\,k^2\,\mathrm{Re}(\theta,\overline{\varphi}).\end{aligned} \tag{B.11}$$

We rewrite (B.11) in the following way,

$$\begin{aligned}(k^4|\sqrt{z}\varphi|^2 + 2k^2|\sqrt{z}\varphi'|^2 + |\sqrt{z}\varphi''|^2) + L(|\sqrt{z}\psi'|^2 + k^2|\sqrt{z}\psi|^2) \\ + K(k^4|\sqrt{z}\varphi|^2 + 2k^2|\sqrt{z}\varphi'|^2 + |\sqrt{z}\varphi''|^2 + 2((z\psi',\overline{\varphi}') + (z\varphi',\overline{\psi}'))) \\ + 2k^2((z\psi,\overline{\varphi}) + (z\varphi,\overline{\psi})) + 4|\sqrt{z}\psi|^2 + 2((\psi,\overline{\varphi}') + (\varphi',\overline{\psi}))) \\ = \mathrm{Ra}\,k^2\,\mathrm{Re}(\theta,\overline{\varphi}).\end{aligned}$$

This last relation can be rewritten as

$$|\sqrt{z}\Phi|^2 + K|\sqrt{z}(\Phi+2\psi)|^2 + L(|\sqrt{z}\psi'|^2 + k^2|\sqrt{z}\psi|^2) = \mathrm{Ra}\, k^2 \,\mathrm{Re}(\theta,\overline{\varphi}), \tag{B.12}$$

where we used the notation $\Phi = k^2\varphi - \varphi''$. From (B.12), we obtain

$$|\sqrt{z}\Phi|^2 + Lk^2|\sqrt{z}\psi|^2 + K((1-\varepsilon)|\sqrt{z}\Phi|^2 + 4\left(1-\frac{1}{\varepsilon}\right)|\sqrt{z}\psi|^2) \leq \mathrm{Ra}\, k^2 \,\mathrm{Re}(\theta,\overline{\varphi}), \tag{B.13}$$

where we used the identity

$$|\sqrt{z}(\Phi+2\psi)|^2 = |\sqrt{z}\Phi|^2 + 4|\sqrt{z}\psi|^2 + 2((z\Phi,\overline{\psi}) + (z\psi,\overline{\Phi}))$$

and the Young inequality

$$-\varepsilon|\sqrt{z}\Phi|^2 - \frac{4|\sqrt{z}\psi|^2}{\varepsilon} \leq 2((z\Phi,\overline{\psi}) + (z\psi,\overline{\Phi})).$$

As $k \geq 1$, we can rewrite the relation (B.13) as follows

$$(1+K(1-\varepsilon))|\sqrt{z}\Phi|^2 + \left(4K\left(1-\frac{1}{\varepsilon}\right) + L\right)|\sqrt{z}\psi|^2 \leq \mathrm{Ra}\, k^2 \,\mathrm{Re}(\theta,\overline{\varphi}). \tag{B.14}$$

The last term on the left-hand-side of (B.14) vanishes for

$$\varepsilon = \frac{4K}{4K+L}.$$

For such ε, we obtain, taking into account the definition of Φ,

$$\frac{4K+L+KL}{\mathrm{Ra}(4K+L)}\left(k^2|\sqrt{z}\varphi|^2 + 2|\sqrt{z}\varphi'|^2 + \frac{1}{k^2}|\sqrt{z}\varphi''|^2\right) \leq \mathrm{Re}(\theta,\overline{\varphi}).$$

By the Cauchy inequality, we obtain

$$\frac{2}{\widetilde{\mathrm{Ra}}}(|\sqrt{z}\varphi|\,|\sqrt{z}\varphi''| + |\sqrt{z}\varphi'|^2) \leq \mathrm{Re}(\theta,\overline{\varphi}), \tag{B.15}$$

where

$$\widetilde{\mathrm{Ra}} = \mathrm{Ra}\,\frac{4K+L}{4K+L+KL}. \tag{B.16}$$

The relation (B.15) is the same as the inequality above (A.10) on p. 239 in [10] with Ra replaced with $\widetilde{\mathrm{Ra}}$. This means that $\widetilde{\mathrm{Ra}}$ plays the same role as Ra in further computations. The remaining part of the proof of Theorem 1 closely follows [10], therefore we postpone it until the Appendix C.

Appendix C. Proof of Theorem 1

In this section we provide the proof of the Theorem 1, which follows the same scheme as that already presented in [10]. In the proof we focus on the differences between our argument and that of [10].

LEMMA 3. *If $0 < a < b < \infty$, the smooth function u_z satisfies*

$$u_z(a) = u_z(b) = 0, \qquad u_z'(a) = u_z'(b) = 0 \tag{C.1}$$

and $\theta(z)$ is defined by (B.4), then

$$\mathrm{Re} \int_a^b \frac{\theta \overline{u_z}}{z}\, dz \geq \frac{2}{\widetilde{\mathrm{Ra}}} \int_a^b \frac{|u_z'|^2}{z}\, dz \geq \frac{2}{\widetilde{\mathrm{Ra}}} \int_a^b \frac{|u_z|^2}{z^3}\, dz. \tag{C.2}$$

Proof. The fundamental estimate in the proof is the relation (B.15). With this relation the argument exactly follows the lines of the proof in the Appendix of [10]. □

In the derivation of (B.15) in Appendix 6 the presence of the singularity in $z = 0$ requires attention. For the moment, we held z. This problem needs to be dealt with, in order to apply the inequality (C.2) to our problem. The treatment of the replacement choice $z + \varepsilon$ and the limit $\varepsilon \to 0$ in terms of integrability of the functions is the key idea on the next Corollary, and exactly follows the lines of the corresponding result in [10].

COROLLARY 4. *Assume that $\theta(z) \in L^2(0,1)$ and u_z satisfy* (B.4)–(B.6). *Moreover, assume that*

$$|u_z(z)| \leq C z^2, \tag{C.3}$$

with the constant C dependent of Ra*, k^2, K, L, and $|\theta|$. Then there holds the bound*

$$\mathrm{Re} \int_0^1 \frac{\theta \overline{u_z}}{z}\, dz \geq \frac{2}{\widetilde{\mathrm{Ra}}} \int_0^1 \frac{|u_z|^2}{z^3}\, dz. \tag{C.4}$$

Proof. We skip the proof as it is identical to that of [10], see p. 237 in that article. □

Now, we prove relation (C.3). The proof relies on finding the bound on $|u_z''''|$. We write the proof in details, since, in contrast to [10], the estimate cannot be derived in one step, it is needed to use the estimate of $|u_z''|$ in the proof.

COROLLARY 5. *Let the complex valued function u_z satisfy* (B.4)–(B.6) *with the corresponding $\theta \in L^2(0,1)$ and ζ. Then there holds the bound* (C.3) *with the constant C dependent of* Ra, $|k|^2$, L, K, *and* $|\theta|$.

Proof. For every $k \in \mathbb{N} \setminus \{0\}$ let us write

$$|\operatorname{Re} u_z(z)| = \left| \int_0^z dz' \int_0^{z'} dz'' \operatorname{Re} u_z''(z'') \right| \le \frac{1}{2} z^2 \|\operatorname{Re} u_z''\|_{L^\infty},$$

$$|\operatorname{Im} u_z(z)| = \left| \int_0^z dz' \int_0^{z'} dz'' \operatorname{Im} u_z''(z'') \right| \le \frac{1}{2} z^2 \|\operatorname{Im} u_z''\|_{L^\infty}.$$

As $\operatorname{Re} u_z$ and $\operatorname{Im} u_z$ are the smooth real valued function satisfying both homogeneous Dirichlet and Neumann boundary conditions on $(0,1)$ by the interpolation Lemma of [9] it follows that

$$\|\operatorname{Re} u_z''\|_{L^\infty} \le \sqrt{2|\operatorname{Re} u_z''''|\,|\operatorname{Re} u_z''|} \text{ and } \|\operatorname{Im} u_z''\|_{L^\infty} \le \sqrt{2|\operatorname{Im} u_z''''|\,|\operatorname{Im} u_z''|}. \tag{C.5}$$

We deduce that

$$|u_z(z)| \le C z^2 \sqrt{|u_z''|\,|u_z''''|}.$$

Hence, to get the required estimate we need to get the L^2 norm bounds for the second and fourth order derivatives of u_z. We first derive the bound of u_z''. To this end we test (B.4) by $\overline{u_z}$ and (B.5) by $\overline{\zeta}$ and we perform integration by parts on the interval $(0,1)$. It follows that

$$\begin{aligned} &k^4|u_z|^2 + 2k^2|u_z'|^2 + |u_z''|^2 \\ &\qquad + K(k^4|u_z|^2 - 2k^2(u_z'', \overline{u_z}) + |u_z''|^2 + 2(k^2\zeta - \zeta'', \overline{u_z})) = \operatorname{Ra} k^2(\theta, \overline{u_z}), \\ &L(k^2|\zeta|^2 + |\zeta'|^2) + K(4|\zeta|^2 + 2(k^2 u_z - u_z'', \overline{\zeta})) = 0. \end{aligned}$$

Adding the two equations, we obtain after obvious computations

$$k^4|u_z|^2 + 2k^2|u_z'|^2 + |u_z''|^2 + L(k^2|\zeta|^2 + |\zeta'|^2) + K|k^2 u_z - u_z'' + 2\zeta|^2 = \operatorname{Ra} k^2(\theta, \overline{u_z}).$$

We deduce that

$$k^4|u_z|^2 + 2k^2|u_z'|^2 + |u_z''|^2 + L(k^2|\zeta|^2 + |\zeta'|^2) \le \frac{k^4}{2}|u_z|^2 + \frac{\operatorname{Ra}^4}{2}|\theta|^2.$$

It follows that

$$|u_z| + |u_z'| + |u_z''| + |\zeta| + |\zeta'| \le C, \tag{C.6}$$

where the constant C depends on $|\theta|, \mathrm{Ra}, L$, and k. Now, multiplying (B.5) by the adjoint of this equation and integrating over the interval $(0,1)$ implies

$$L(k^2\zeta - \zeta'', k^2\overline{\zeta} - \overline{\zeta''}) = 4K^2(2\zeta + k^2 u_z - u_z'', 2\overline{\zeta} + k^2\overline{u_z} - \overline{u_z''}).$$

We deduce that

$$k^4|\zeta|^2 + |\zeta''|^2 + 2k^2|\zeta'|^2 = \frac{4K^2}{L}(4|\zeta|^2 + k^4|u_z|^2 + |u_z''|^2 + 4k^2\mathrm{Re}\,(\zeta, \overline{u_z}) - 4\mathrm{Re}\,(\zeta, \overline{u_z''}) + 2k^2|u_z'|^2).$$

Hence

$$|\zeta''|^2 \le \frac{4K^2}{L}(4|\zeta|^2 + k^4|u_z|^2 + |u_z''|^2 + 4k^2|\zeta|\,|u_z| + 4|\zeta|\,|u_z''| + 2k^2|u_z'|^2).$$

Using (C.6) we deduce that

$$|\zeta''| \le C,$$

where now C depends on $|\theta|, \mathrm{Ra}, L, K$, and k. This control is necessary in order to bound the fourth order derivative of u_z in L^2. Finally, multiplying (B.4) by its adjoint and integrating we obtain

$$(1+K)^2(k^4 u_z - 2k^2 u_z'' + u_z'''', k^4\overline{u_z} - 2k^2\overline{u_z''} + \overline{u_z''''}) = (\mathrm{Ra}\,k^2\theta - 2K(k^2\zeta - \zeta''), \mathrm{Ra}\,k^2\overline{\theta} - 2K(k^2\overline{\zeta} - \overline{\zeta''})).$$

It is clear that all terms in the right-hand side are bounded by a constant C. Hence

$$(k^4 u_z - 2k^2 u_z'' + u_z'''', k^4\overline{u_z} - 2k^2\overline{u_z''} + \overline{u_z''''}) \le C.$$

Multiplying and integrating by parts we obtain

$$k^8|u_z|^2 + 4k^4|u_z''|^2 + |u_z''''|^2 + 2k^4|u_z''|^2 + 4k^6|u_z'|^2 \le C + 4k^2\mathrm{Re}\,(u_z'', \overline{u_z''''}).$$

We use (C.6) to deduce

$$|u_z''''|^2 \le C + 4k^2 C|u_z''''|.$$

It follows that $|u_z''''| \le C$ and the proof is complete. □

Now, in order to obtain the bound for the Nusselt number we proceed exactly in the same framework as [10] introducing the so-called logarithmic background profile. More precisely, let $\delta \in (0, 1/2)$ be the boundary layer thickness and define

$$\tau(z) = \begin{cases} 1 - \frac{z}{\delta} & 0 \le z \le \delta, \\ \frac{1}{2} + \lambda(\delta)\ln\left(\frac{z}{1-z}\right) & \delta \le z \le 1-\delta, \\ \frac{(1-z)}{\delta} & 1-\delta \le z \le 1, \end{cases} \tag{C.7}$$

where

$$\lambda(\delta) = \frac{1}{2\ln((1-\delta)/\delta)}.$$

The Dirichlet integral of $\tau'(z)$ can be evaluated as

$$\int_0^1 |\tau'(z)|^2\,dz = \frac{2}{\delta}\left(1 + \frac{\delta}{2\ln\frac{1-\delta}{\delta}} + \frac{1}{4\ln^2\frac{1-\delta}{\delta}}\left(1 - \frac{\delta}{1-\delta}\right)\right). \tag{C.8}$$

In particular, if $\delta \le 1/4$ then

$$\int_0^1 |\tau'(z)|^2\,dz \le \frac{2}{\delta}\left(1 + \frac{1}{8\ln 3} + \frac{1}{6\ln^2 3}\right) \le \frac{3}{\delta}. \tag{C.9}$$

REMARK 6. The relation (C.8) actually states that

$$\int_0^1 \left|\tau'(z)\right|^2 dz = \frac{2}{\delta}(1 + C(\delta)),$$

where $C : [0,\infty) \to [0,\infty)$ is a continuous function such that $\lim_{\delta\to 0} C(\delta) = 0$, so, by taking appropriately small δ one can make the constant on the right-hand side of (C.9) arbitrarily close to $\frac{2}{\delta}$.

The key point now is to show that for a flow having a given Rayleigh number higher than a threshold value, we can choose $\delta \le 1/4$ such that the constraint (5.17) holds. That value of δ gives the bound through (C.8). After some algebra, which follows the lines of the argument on page 234 of [10], (5.17) holds if only

$$\int_0^\delta z^4\left(\frac{1}{\delta} + \frac{\lambda}{z} + \frac{\lambda}{1-z}\right)^2 dz \le \frac{4\lambda}{\widetilde{\mathrm{Ra}}}. \tag{C.10}$$

A straightforward but cumbersome computation yields that if $\delta \le 1/4$, then

$$\int_0^\delta z^4\left(\frac{1}{\delta} + \frac{\lambda}{z} + \frac{\lambda}{1-z}\right)^2 dz \le \frac{\delta^3}{5}\left(1 + \frac{19}{12\ln 3} + \frac{47}{72\ln^2 3}\right) \le \frac{3\delta^3}{5}. \tag{C.11}$$

REMARK 7. In fact we can prove that

$$\int_0^\delta z^4\left(\frac{1}{\delta} + \frac{\lambda}{z} + \frac{\lambda}{1-z}\right)^2 dz \le \frac{\delta^3}{5}(1 + C(\delta)),$$

where $C : [0, \infty) \to [0, \infty)$ is a continuous function such that $\lim_{\delta \to 0} C(\delta) = 0$, so, by taking appropriately small δ one can make the constant on the right-hand side of (C.11) arbitrarily close to $\delta^3/5$.

Now, a sufficient condition for the (C.10) to hold is

$$\widetilde{\mathrm{Ra}}\,\delta^3 \leq \frac{20}{3}\lambda = \frac{10}{3\ln((1-\delta)/\delta)}.$$

If only $\ln \widetilde{\mathrm{Ra}} \leq 5\widetilde{\mathrm{Ra}}$ (which always holds for $\widetilde{\mathrm{Ra}} \geq 1$) this condition is satisfied by

$$\delta = \left(\frac{5}{\widetilde{\mathrm{Ra}} \ln \widetilde{\mathrm{Ra}}}\right)^{1/3}.$$

Note that the restriction $\delta \leq 1/4$ implies that $\widetilde{\mathrm{Ra}} \ln \widetilde{\mathrm{Ra}} \geq 320$ which always holds if, for example, $\widetilde{\mathrm{Ra}} \geq 75$. Substituting the expression for δ into (C.9) we arrive at the result

$$\mathrm{Nu} \leq \int_0^1 |\tau'(z)|^2\, dz \leq \frac{3}{\sqrt[3]{5}}\, \widetilde{\mathrm{Ra}}^{1/3} \ln^{1/3} \widetilde{\mathrm{Ra}}, \tag{C.12}$$

valid if $\widetilde{\mathrm{Ra}} \geq 75$. Using (B.16) yields the assertion of Theorem 1.

We end with final remarks on a possible improvement of the numerical values of constants in the Nusselt number bound provided in the Theorem 1.

REMARK 8. Neither the constant $3/\sqrt[3]{5}$ nor the Rayleigh number bound 75 are optimal. We only present here the example-case computation which leads to the required estimate. It is further possible to relate the constant with the Rayleigh number bound. If the bound is higher then the constant in the Nusselt number estimate becomes smaller. The smallest value of this constant has been given in [10] and is equal to $2/\sqrt[3]{30}$. The constant $3/\sqrt[3]{5}$ is determined by somewhat arbitrary choice of threshold value of δ equal to $1/4$. In general, the smaller bound for δ we choose, the higher threshold $\widetilde{\mathrm{Ra}}$ needs to be, and the lower constant is obtained in place of $3/\sqrt[3]{5}$. We could proceed exactly as in [10] and choose arbitrarily small $\delta > 0$. This would give us the asymptotic result valid for $\widetilde{\mathrm{Ra}} \to \infty$ with the optimal constant $2/\sqrt[3]{30}$ in place of $3/\sqrt[3]{5}$. Since our aim is to demonstrate the influence of micropolar constants L and N on the Nusselt number bound for finite $\widetilde{\mathrm{Ra}}$, in contrast to [10], we decide to present the derivation for a fixed nonzero δ.

REMARK 9. The logarithmic prefactor in (C.12) is raised to the power $1/3$. It is possible to use the techniques of [21] to get the prefactor $\ln^{1/15} \mathrm{Ra}$ by appropriate modification of the background temperature method. We leave as

an open problem if the maximal regularity method which leads in [21] to the doubly logarithmic prefactor can be adapted to the micropolar setting.

References

1. N.A.M. Al-Juma, A.J. Chamkha, *Coupled heat and mass transfer by natural convection of a micropolar fluid flow about a sphere in porous media with Soret and Dufour effects*, in: M.K. Jha, M. Lazard, A. Zaharim, K. Sopian [eds.], *Recent Advances in Fluid Mechanics, Heat & Mass Transfer and Biology*, pp. 204–209, WSEAS Press, Harvard, Cambridge, 2012.
2. T. Ariman, M.A. Turk, N.D. Sylvester, *On steady and pulsatile flow of blood*, Journal of Applied Mechanics, **41**, 1–7, 1974.
3. C. Auth, D. Bercovici, U.R. Christensen, *Two-dimensional convection with a self-lubricating, simple-damage rheology*, Geophysical Journal International, **154**, 783–800, 2003.
4. O. Aydin, I. Pop, *Natural convection in a differentially heated enclosure filled with a micropolar fluid*, International Journal of Thermal Sciences, **46**, 963–969, 2007.
5. A.Y. Bakier, *Natural convection heat and mass transfer in a micropolar fluid-saturated non-Darcy porous regime with radiation and thermophoresis effects*, Thermal Sciience, **15**, S317–S326, 2011.
6. G. Bourantas, V. Loukopoulos, *Modeling the natural convective flow of micropolar nanofluids*, International Journal of Heat and Mass Transfer, **68**, 35–41, 2014.
7. P. Constantin, C. Doering, *Heat transfer in convective turbulence*, Nonlinearity, **9**, 1049–1060, 1996.
8. C. Doering, J. Gibbon, *Applied Analysis of the Navier–Stokes equations*, Cambridge Texts in Applied Mathematics, 1995.
9. C.R. Doering, P. Constantin, *On upper bounds for infinite Prandtl number convection with or without rotation*, Journal of Mathematical Physics, **42**, 784–795, 2001.
10. C.R. Doering, F. Otto, M.G. Reznikoff, *Bounds on vertical heat transport for infinite-Prandtl-number Rayleigh–Bénard convection*, Journal od Fluid Mechanics, **560**, 229–241, 2006.
11. A. Eringen, *Theory of micropolar fluids*, Journal of Mathematics and Mechanics, **16**, 1–16, 1966.
12. A. Grossmann, D. Lohse, *Scaling in thermal convection: a unifying theory*, Journal of Fluid Mechanics, **407**, 27–56, 2000.
13. A. Grossmann, D. Lohse, *Thermal convection for large Prandtl numbers*, Physical Review Letters, **86**, 3316–3319, 2001.
14. Capd library., http://capd.ii.uj.edu.pl.
15. P. Kalita, J.A. Langa, G. Łukaszewicz, *Micropolar meets Newtonian. The Rayleigh–Bénard problem*, Physica D: Nonlinear Phenomena, **392**, 57–80, 2019, DOI: 10.1016/j.physd.2018.12.004.

16. S. KURGIN, J.M. DASCH, D.L. SIMON, G.C. BARBER, Q. ZOU, *Evaluation of the convective heat transfer coefficient for minimum quantity lubrication (MQL)*, Industrial Lubrication and Tribology, **64**, 376–386, 2012.

17. G. ŁUKASZEWICZ, *Micropolar Fluids – Theory and Applications*, Birkhäuser Basel, 1999.

18. W.V.R. MALKUS, *Discrete transitions in turbulent convection*, Proceedings of the Royal Society of London A, **225**, 185–195, 1954.

19. W.V.R. MALKUS, *The heat transport and spectrum of thermal turbulence*, Proceedings of the Royal Society of London A, **225**, 196–212, 1954.

20. M.A.M. NETO, R.M. FRANCA, J.R. BARBAROSA, JR., *Convection-driven absorption of R-1234yf in lubricating oil*, International Journal of Refrigeration, **44**, 151–160, 2014.

21. F. OTTO, C. SEIS, *Rayleigh–Bénard convection: Improved bounds on the Nusselt number*, Journal of Mathematical Physics, **52**, 083702, 2011.

22. R.C. SHARMA, P. KUMAR, *Effect of rotation on thermal convection in micropolar fluids in porous medium*, Indian Journal of Pure and Applied Mathemathics, **29**, 95–104, 1998.

23. R.J.A.M. STEVENS, E.P. VAN DER POEL, S. GROSSMANN, D. LOHSE, *The unifying theory of scaling in thermal convection: updated prefactors*, Journal of Fluid Mechanics, **730**, 295–308, 2013.

24. X. WANG, *Asymptotic behavior of the global attractors to the boussinesq system for Rayleigh–Bénard convection at large Prandtl number*, Communications on Pure and Applied Mathematics, **60**, 1293–1318, 2007.

25. S. WRENICK, P. SUTOR, H. PANGILINAN, E.E. SCHWARZ, *Heat transfer properties of engine oils*, [in:] Proceedings of the World Tribology Congress III, Washington, D.C., USA, 2005.

Received June 19, 2020; revised version October 05, 2020.
Published online December 17, 2020.